

Facile one step synthesis and gas sensing behavior of PANI/Mn₃O₄ nanocomposite

Anupma Sharma, Vijay Kumar, Saurav Kumar, Pooja D., Sudeshna Bagchi, Amol P. Bhondekar*

Agrionics, CSIR-Central Scientific Instruments Organisation, Sector-30 C, Chandigarh, 160030, India

*Corresponding author: Tel: (+91)17-22651787; E-mail: amol.bhondekar@gmail.com, amolbhondekar@csio.res.in

Received: 17 March 2016, Revised: 30 September 2016 and Accepted: 07 November 2016

DOI: 10.5185/amp.2017/710
www.vbripress.com/amp

Abstract

In this work, we present the first investigations of Mn₃O₄ nanoparticles doped in polyaniline (PANI) matrix for gas sensing application. PANI/Mn₃O₄ nanocomposite (NC) was synthesized by facile one step reduction method with varied dopant concentrations (1mM and 3mM) of synthesized Mn₃O₄ nanoparticles followed by its characterization for optical, structural, morphological, thermal and electrical properties. Optical characterization by UV-Vis and FT-IR confirmed the doping of Mn₃O₄ in polymer matrix. TGA analysis showed improvement in the thermal stability of the NC. SEM images portrayed agglomerated morphology of PANI whereas the NC depicted fibre-like structures symptomatic of more porosity. Gas sensing behavior was investigated towards acetone, ethanol and benzaldehyde vapours. The sensor with 3mM dopant concentration exhibited significant sensing response with a sensitivity of 1.5 at room temperature towards acetone vapour, which can be attributed to the controlled and improved properties at the interface via molecular and supramolecular interactions. The synthesized NC has a potential use as acetone sensor with fast response and recovery. Copyright © 2017 VBRI Press.

Keywords: PANI, Mn₃O₄, nanocomposite, gas sensing, acetone.

Introduction

Colossal demand for the gas sensors in the industrial, biomedical, food, automotive sectors etc. have prompted the researchers for the exploration of novel materials. In this regard, during the last decades much attention has been paid on the metal oxide and conducting polymer based gas sensors [1-3]. Both of the gas sensing techniques has its intrinsic limitations and diverse applicability. Generally, sensors based on metal/metal oxide semiconductors have been proven widely effective for inorganic vapors. Also, the high operation temperature of the metal oxide sensors demands high cost and complicated configurations which are the major drawbacks of this type of sensors. Whereas, the conducting polymer based sensors have been reported more sensitive for the detection of extensive range of volatile organic compounds (VOC) [2] at ambient temperature which makes them attractive candidate as gas sensing elements. Actually, the electrical and optical properties of the conducting polymers are different from the conventional system which is due to presence of highly delocalized and easily polarizable π - electrons. Although, the conductivity of pure polymer is too low to act as a sensing material but it can be improved by doping the polymer chemically, electrochemically, through redox reaction, photo chemically, etc. or by adding some fillers such as carbon black, metal particles, carbon fibers or aluminium flakes, etc. [4].

Conducting polymers such as polyaniline (PANI), polypyrrole (PPy), polythiophene (PT), poly(*p*-phenylene) (PPP), etc. are the basic conducting polymers having conductivity range from 3.0 to 10⁵ Scm⁻¹ and optical absorption edge from 1.5-3.2 eV [4].

Among conducting polymers, PANI has been investigated widely due to its remarkable overall properties, for instance, low cost, simple synthesis & granular metals like behavior [5]. It has wide application in the area of microelectronic devices, light weight batteries [6, 7], sensors [8, 9], supercapacitors [10], microwave absorption [11], corrosion inhibition [12], catalysis [13] etc. Various metal oxides such as TiO₂ [14], SnO₂ [15], In₂O₃ [16], MoO₃ [17], WO₃ [18], NiO [19], chalcogenides [20], etc. nanoparticles have been doped with PANI to enhance its unique physical properties. Recently, electrical and magnetic behavior of PANI/Mn₃O₄ has been reported [21]. However, Mn₃O₄ doped PANI has not been explored yet for gas-sensing except its application as humidity sensor [22].

In this work, a simple and novel approach has been adopted for the synthesis PANI/Mn₃O₄ nanocomposites by an in-situ polymerization. In addition, influence of dopant concentration on the gas-sensing properties of PANI nanocomposite (NC) has been investigated for three VOCs viz. acetone, ethanol and benzaldehyde.

Experimental

Materials

All the reagents used were of analytical grade. Potassium permanganate (KMnO_4) and monohydrate hydrazine (NH_2NH_2) were purchased from Qualigens Fine Chemicals, Mumbai. N-cetyl-N, N, N-trimethyl ammoniumbromide(CTAB), Tetrabutylammonium bromide(TBAB), aniline, ammonium peroxy sulfate (APS), acetone and benzaldehyde were purchased from Loba Chemie, Mumbai whereas ethanol was procured from Fisher Scientific, UK. Aqueous solutions were prepared from the double distilled water having resistance $10^{18}\Omega$.

Material synthesis

Firstly, Mn_3O_4 nanoparticles were synthesized by our earlier reported protocol [23]. In brief, 0.5 mmol of CTAB, 0.1 mmol TBAB and 0.5 mmol of KMnO_4 were mixed together with 100 ml of water in a round bottom flask. The reaction mixture was allowed to get homogenized for 10 minutes under slow stirring in order to avoid froth formation. Further, 0.5 mmol of NH_2NH_2 was added rapidly to this solution under vigorous magnetic stirring. The color of the reaction mixture changed from dark purple to dark brown and finally to brown with a tinge of orange. It was further heated to 70°C for 1 hr and then cooled to room temperature resulting in complete precipitation. The precipitate was separated by centrifugation followed by several washing cycles with ethanol and then dried in vacuum for three hrs at 40°C .

In order to synthesize PANI/ Mn_3O_4 composite, two different concentrations (1.0 mM and 3.0 mM) of synthesized Mn_3O_4 nanoparticles were prepared in 20.0 ml of HCl (0.2 M) solution. Then, $91.3\ \mu\text{l}$ of aniline was added to the each Mn_3O_4 solution and kept for stirring for an hour. Another solution of the oxidant APS (0.285 g) in HCl (0.2 M) was prepared. Then, this oxidant solution was added drop wise to the aniline and Mn_3O_4 solution and kept for stirring for an hour. The resultant products were filtered, washed with acetone, DI and dried at 24°C .

Sample preparation for SEM analysis

Thin films of the PANI and PANI/ Mn_3O_4 were developed using spin coating technique. 5 mg of sample was dissolved in NMP (100 μl) and kept for stirring for 3-4 hrs. Then, thin films were prepared using spin coating (Millman, single stage coating unit) at the 1200 rpm for 15 sec.

Characterizations

The different instruments used for the characterization of samples included a UV-Vis spectrophotometer (UV-Vis-NIR, Varian Cary 5000), Fourier-transform infrared spectroscope (FTIR, Perkin Elmer), thermo gravimetric analyzer (TGA, Thermo Scientific) and field-emission scanning electron microscopy (FESEM, Hitachi S4800).

Gas sensing set up & response measurements

Test samples to be used as a sensor were prepared in the pellet form. Compressed pellets of specimens were prepared under the hydraulic pressure of 10 psi load. A chromel/alumel sensing wire was inserted in each pellet. All the pellets were 15.0 mm in diameter and 0.92 mm in thickness. The gas sensing measurements were carried out in a customized testing set-up [24], using Agilent B2901A source-measure unit. Different concentrations of analyte vapours in the range of 1.0 ppm-100.0 ppm were injected in the test chamber and the corresponding sensor response was measured. The sensitivity(S) was calculated using the following equation:

$$S = \frac{R_g}{R_0} - 1$$

where, R_g = Saturated maximum resistance in the presence of analyte, R_0 = Baseline resistance of the sensor.

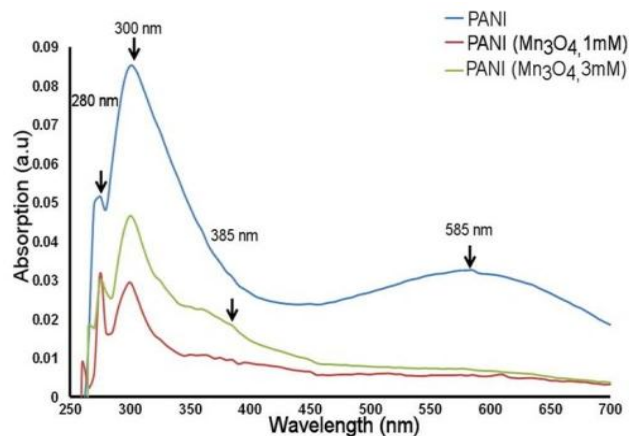


Fig. 1. UV-Vis spectral overlay of PANI & PANI/ Mn_3O_4 (1 mM, 3 mM).

Results and discussion

UV-Vis analysis

The UV/vis spectra of PANI and PANI/ Mn_3O_4 were recorded in N-methylpyrrolidone (NMP) as solvent and presented in Fig. 1. The absorbance maximas seen at 275 nm and 300 nm are due to the π - π^* transition of benzenoid ring and the maxima at 585 nm corresponds to the polaron $-\pi^*$ transition [25]. Whereas, in case of NCs a new band appears at 370 nm, which corresponds to the highest occupied molecular orbital of the benzenoid to the lowest unoccupied molecular orbital of the localized quinoid ring and the two-surrounding imine nitrogens in the emeraldine base form of PANI (π - π^* transition) [26]. Also peak at 585 nm diminished and an additional shoulder appeared at wavelength lower than 275 nm, which can be attributed to the successful interaction of metal oxide with the polymer chain.

SEM analysis

Fig. 2 shows the SEM morphology of PANI and PANI/Mn₃O₄ thin film. It indicates that PANI/Mn₃O₄ possess a very porous structure with an interconnected network of nanofibers. However, PANI has a rough surface including two-dimensional slab surface. Porous structure of NC may affect the diffusion of gas molecules which is beneficial for the gas sensor application due to their highly specific surface and excellent channels for charge transmission [27, 28]. It is believed that, during the polymerization of PANI, Mn₃O₄ nanoparticles in the reaction system play a role as reaction core, resulting in the adsorption of monomer on the surface of nanoparticles and on overgrown growth around these particles [29].

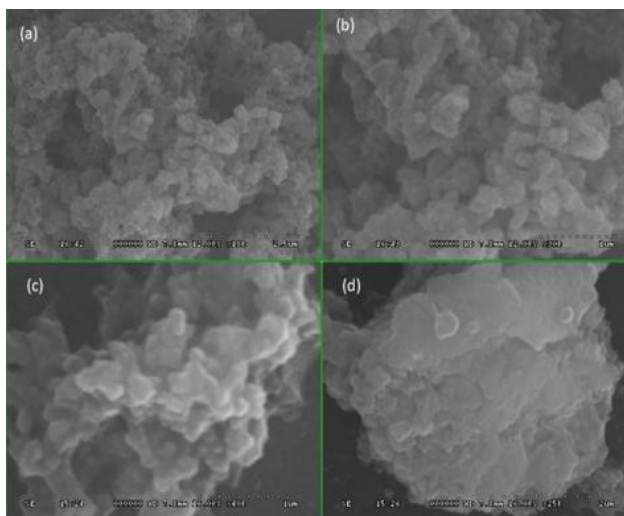


Fig. 2: SEM images of (a) PANI/Mn₃O₄ (× 18 k); (b) PANI/Mn₃O₄ (× 12.0 k); (c) PANI (× 40 k); (d) PANI (× 25 k).

FT-IR analysis

The FTIR spectrum of PANI and PANI/Mn₃O₄ (1 mM, 3 mM) is depicted in **Fig. 3** and the observed bands are described in **Table 1**.

Table 1. FT-IR peak assignment.

PANI	PANI/Mn ₃ O ₄ (cm ⁻¹)	Type of Stretching
-	410.7	Mn _{octahedral} -O stretching ^[31]
-	514.9, 619.0	Coupling between Mn _{octahedral} -O & Mn _{tetrahedral} -O stretching modes ^[32-33]
819.5	819.5	C-H out of plane bending vibrations ^[30]
1261.2	1261.2	C-N stretching of the benzenoid ring ^[34]
1475.2	1471.4	C=C stretching vibration of benzenoid ring ^[34]
1558.2	1550.9	C=C stretching vibration of quinoid ring ^[34]

FTIR spectra of PANI show the main characteristic peaks at 1558.2, 1475.2, 1261.2 and 819.5 cm⁻¹. The bands at 1558.2 and 1475.2 cm⁻¹ are attributed to stretching vibrations of N=Q=N ring and N-B-N ring respectively (where B refers to benzenoid-type rings and Q refers to quinoid-type rings). The bands at 1261.2 cm⁻¹ correspond to the symmetric component of the C-C stretching modes. The peak at 819.5 cm⁻¹ can be

attributed to the out-of-plane bending vibration of C-H on the 1, 4-disubstituted aromatic rings [19].

The characteristic peaks of Mn₃O₄ (410.7, 514.9, and 619.0 cm⁻¹) are observed in the spectra of PANI/Mn₃O₄. The transmittance bands due to stretching vibrations of quinoid (1550.9 cm⁻¹) and benzenoid (1471.4 cm⁻¹) rings in PANI/Mn₃O₄ confirmed the polymerization of aniline in the presence of Mn₃O₄. The interaction between PANI and Mn₃O₄ nanoparticles was confirmed as these bands were found to be shifted to lower wavelengths as well the intensity of the bands was diminishing.

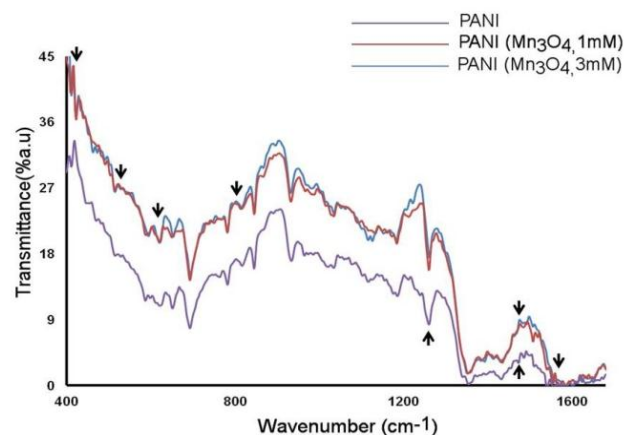


Fig. 3. FT-IR spectral overlay of PANI & PANI/Mn₃O₄ (1 mM, 3 mM).

TGA analysis

Thermal analysis of PANI and PANI/Mn₃O₄ in the temperature range of 30°C to 1000°C in N₂ atmosphere reveals two gradual weight loss transition phases corresponding to moisture loss and decomposition of organic matter (**Fig. 4**). The degradation of PANI/Mn₃O₄ begins at a much lower temperature. This behavior could be originated from the fact that Mn₃O₄ particles behave as catalysts, thus reducing the degradation temperature of PANI [35].

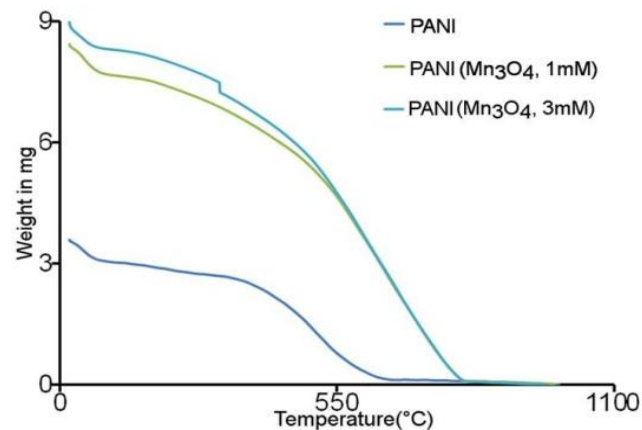


Fig. 4: TGA thermogram of PANI & PANI/Mn₃O₄ (1 mM, 3 mM).

Also, as the concentration of the dopant is increasing (**Fig. 4**), the degradation temperature is also increasing (810-860°C). The improvement in the thermal stability for

the PANI/Mn₃O₄ is attributed to the interaction between PANI and Mn₃O₄. This interaction restricts the thermal motion of PANI chains and shields the degradation of PANI in the NCs [30].

Gas sensing results

The dynamic gas sensing response characteristics of the PANI/Mn₃O₄ (1 mM) & PANI/Mn₃O₄ (3 mM) doped sensor at room temperature are shown in Fig. 5(a) & 5(b) respectively. It can be observed that the resistance of both the sensors decreases dramatically after exposed to acetone vapours. PANI/Mn₃O₄ (1 mM) is much less sensitive to acetone than PANI/Mn₃O₄ (3 mM) sensor. Poor & noisy response has been observed towards 60 ppm of acetone vapours in case of Mn₃O₄ (1 mM). The resistance of the sensor decreased on exposure to volatile vapours, which can be attributed to the fact that adsorption of vapour molecules resulted in the increased mobility of dopant ions. On removal of acetone vapours, the sensor quickly recovered back to its baseline resistance.

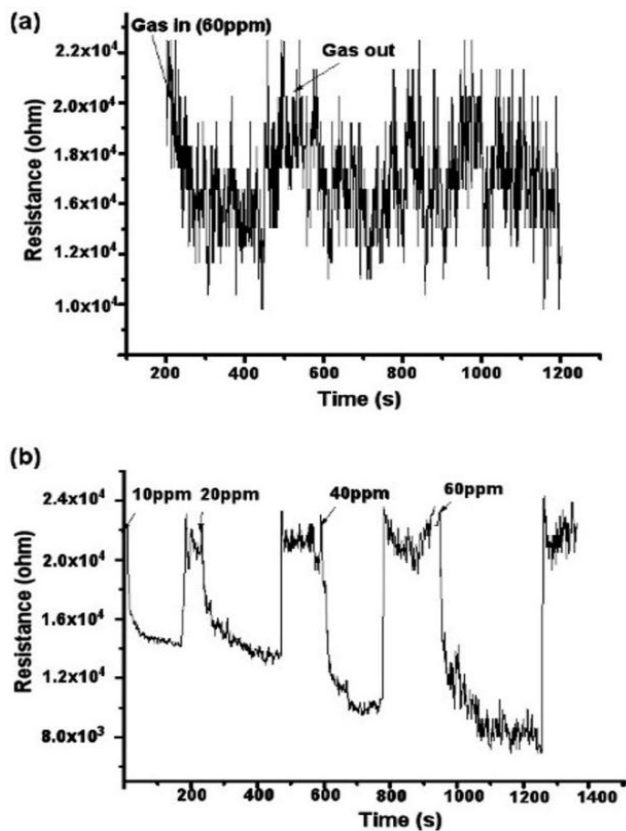


Fig. 5: Dynamic gas response for acetone of (a) PANI/Mn₃O₄ (1 mM) and (b) PANI/Mn₃O₄ (3 mM).

The change in the electrical behavior of the polymer on exposure to any gas can be correlated to the direction of the partial charge transfer and this phenomenon is dependent on the electronegativity of the vapour and work function of the polymer [36]. VOCs may be interacting with the polymer composite via physisorption

mechanisms such as induced dipole/induced dipole interactions (also named London dispersion), dipole/induced dipole interactions, dipole/dipole interactions and hydrogen bonds (Lewis acidity/basicity-concept) [37].

PANI/ Mn₃O₄ (3 mM) has been exposed to acetone, ethanol and benzaldehyde in the concentration range from 10-60 ppm and the dynamic response for the acetone vapours has been depicted in Fig. 5(b). With increase in vapour concentration, sensitivity increases owing to the increased number of adsorbed vapour molecules. Sensitivity for each gas has been plotted in Fig. 6. The sensor with 3 mM dopant concentration exhibited significant sensing response with a sensitivity of 1.5 at room temperature towards acetone vapours. The sensor is highly selective towards acetone vapours as seen in Fig. 6. Thus, the result suggests that this sensor could provide an excellent sensing platform for acetone sensing.

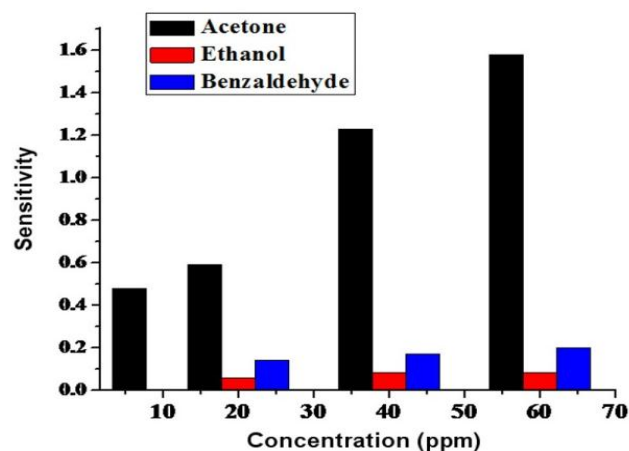


Fig. 6: Sensitivity of PANI/Mn₃O₄ towards acetone, benzaldehyde dan ethanol.

Conclusion

Facile route has been devised for the synthesis of PANI/Mn₃O₄. Effect of dopant on the structural morphology has been demonstrated. PANI/Mn₃O₄ NC has been found to be more porous as compared to undoped PANI which also implicates the more aptness of the NC for gas sensing. This NC formed has been found to be more suitable in terms of electrical conductivity, thermal stability and VOC sensing. The synthesized NC has a promising use as acetone sensor with fast response and recovery.

Acknowledgements

The authors are thankful to Director, CSIO for his kind permission to carry out this work.

Author's contributions

Conceived the plan: AB, AS, SB; Performed the experiments: AS, VK, SK, SB, PD; Data analysis: AS, SK, SB, PD; Wrote the paper: AS, PD, SK, SB, AB. Authors have no competing financial interests.

References

1. Sun, Y. F.; Liu, S.-B.; Meng, F.-L.; Liu, J.-Y.; Jin, Z.; Kong, L.-T.; Liu, J.-H.; *Sens.*, **2012**, *12*, 2610.
DOI: [10.3390/s120302610](https://doi.org/10.3390/s120302610)
2. Liu, X.; Cheng, S.; Liu, H.; Hu, S.; Zhang, D.; Ning, H.; *Sens.*, **2012**, *12*, 9635.
DOI: [10.3390/s120709635](https://doi.org/10.3390/s120709635)
3. Tricoli, A.; Righettoni, M.; Teleki, A.; *Angew. Chem., Int. Ed. Engl.*, **2010**, *49*, 7632.
DOI: [10.1002/anie.200903801](https://doi.org/10.1002/anie.200903801)
4. Dai, L. (Eds.); *Conducting Polymers, In Intelligent Macromolecules for Smart Devices*; Springer-Verlag: UK, **2004**.
DOI: [10.1007/b97517](https://doi.org/10.1007/b97517)
5. Stamenov, P.; Madathil, R.; Coey, J. M. D.; *Sens. Actuators, B*, **2012**, *161*, 989.
DOI: [10.1016/j.snb.2011.11.082](https://doi.org/10.1016/j.snb.2011.11.082)
6. Gurunathan, K.; Amalnerkar, D. P.; Trivedi, D. C.; *Mater. Lett.*, **2003**, *57*, 1642.
DOI: [10.1016/S0167-577X\(02\)01045-5](https://doi.org/10.1016/S0167-577X(02)01045-5)
7. Amado, F. D. R.; Krishnamurthy, S.; *Adv. Mater. Lett.*, **2016**, *7*, 719.
DOI: [10.5185/amlett.2016.6127](https://doi.org/10.5185/amlett.2016.6127)
8. Radhapyari, K.; Khan, R.; *Adv. Mater. Lett.*, **2015**, *6*, 13.
DOI: [10.5185/amlett.2015.5607](https://doi.org/10.5185/amlett.2015.5607)
9. Deng, J.; He, C.; Peng, Y.; Wang, J.; Long, X.; Li, P.; Chan, A. S. C.; *Synth. Met.*, **2003**, *139*, 295.
DOI: [10.1016/S0379-6779\(03\)00166-8](https://doi.org/10.1016/S0379-6779(03)00166-8)
10. Peng, C.; Zhang, S.; Jewell, D.; Chen, G. Z.; *Prog. Nat. Sci.*, **2008**, *18*, 777.
DOI: [10.1016/j.pnsc.2008.03.002](https://doi.org/10.1016/j.pnsc.2008.03.002)
11. Makeiff, D. A.; Huber, T.; *Synth. Met.*, **2006**, *156*, 497.
DOI: [10.1016/j.synthmet.2005.05.019](https://doi.org/10.1016/j.synthmet.2005.05.019)
12. Sathiyarayanan, S.; Karpakam, V.; Kamaraj, K.; Muthukrishnan, S.; Venkatachari, G.; *Surf. Coat. Technol.*, **2010**, *204*, 1426.
DOI: [10.1016/j.surfcoat.2009.09.037](https://doi.org/10.1016/j.surfcoat.2009.09.037)
13. Zhou, Q.; Shi, G.; *J. Am. Chem. Soc.*, **2016**, *138*, 2868.
DOI: [10.1021/jacs.5b12474](https://doi.org/10.1021/jacs.5b12474)
14. Ma, X.; Wang, M.; Li, G.; Chen, H.; Bai, R.; *Mater. Chem. Phys.*, **2006**, *98*, 241.
DOI: [10.1016/j.matchemphys.2005.09.027](https://doi.org/10.1016/j.matchemphys.2005.09.027)
15. Ram, M. K.; Yavuz, Ö.; Lahsangah, V.; Aldissi, M.; *Sens. Actuators, B*, **2005**, *106*, 750.
DOI: [10.1016/j.snb.2004.09.027](https://doi.org/10.1016/j.snb.2004.09.027)
16. Sadek, A. Z.; Wlodarski, W.; Shin, K.; Kaner, R. B.; Kalantar-zadeh, K.; *Nanotechnol.*, **2006**, *17*, 4488.
DOI: [10.1088/09574484/17/17/034](https://doi.org/10.1088/09574484/17/17/034)
17. Wang, J.; Matsubara, I.; Murayama, N.; Woosuck, S.; Izu, N.; *Thin Solid Films*, **2006**, *514*, 329.
DOI: [10.1016/j.tsf.2006.02.030](https://doi.org/10.1016/j.tsf.2006.02.030)
18. Parvatikar, N.; Jain, S.; Khasim, S.; Revansiddappa, M.; Bhoraskar, S. V.; Prasad, M. V. N. A.; *Sens. Actuators, B*, **2006**, *114*, 599.
DOI: [10.1016/j.snb.2005.06.057](https://doi.org/10.1016/j.snb.2005.06.057)
19. Nandapure, B. I.; Kondawar, S. B.; Salunkhe, M. Y.; Nandapure, A. I.; *Adv. Mat. Lett.*, **2013**, *4*, 134
DOI: [10.5185/amlett.2012.5348](https://doi.org/10.5185/amlett.2012.5348)
20. Nguyen, D.; Yoon, H.; *Polymers*, **2016**, *8*, 118.
DOI: [10.3390/polym8040118](https://doi.org/10.3390/polym8040118)
21. Shambharkar, B. H.; Umare, S. S.; Rathod, R. C.; *Trans. Indian Inst. Met.*, **2014**, *67*, 827.
DOI: [10.1007/s12666-014-0405-8](https://doi.org/10.1007/s12666-014-0405-8)
22. Singla, M. L.; Awasthi, S.; Srivastava, A.; *Sens. Actuators, B*, **2007**, *127*, 580.
DOI: [10.1016/j.snb.2007.05.018](https://doi.org/10.1016/j.snb.2007.05.018)
23. Kohli, P. S.; Devi, P.; Reddy, P.; Raina, K. K.; Singla, M. L.; *J. Mater. Sci.: Mater. Electron*, **2012**, *23*, 1891.
DOI: [10.1007/s10854-012-0680-2](https://doi.org/10.1007/s10854-012-0680-2)
24. Kumar, S.; Bagchi, S.; Prasad, S.; Sharma, A.; Kumar, R.; Kaur, R.; Singh, J.; Bhondekar, A. P.; *Beilstein J. Nanotechnol.*, **2016**, *7*, 501.
DOI: [10.3762/bjnano.7.44](https://doi.org/10.3762/bjnano.7.44)
25. Huang, H.; Zeng, X.; Li, W.; Wang, H.; Wang, Q.; Yang, Y. J.; *Mater. Chem. A*, **2014**, *2*, 16516.
DOI: [10.1039/C4TA03332A](https://doi.org/10.1039/C4TA03332A)
26. Alam, M.; Ansari, A. A.; Shaik, M. R.; Alandis, N. M.; *Arabian J. Chem*, **2013**, *6*, 341.
DOI: [10.1016/j.arabjc.2012.04.021](https://doi.org/10.1016/j.arabjc.2012.04.021)
27. Ma, X.; Zhang, X.; Li, Y.; Li, G.; Wang, M.; Chen, H.; Mi, Y.; *Macromol. Mater. Eng.*, **2006**, *291*, 75.
DOI: [10.1002/mame.200500296](https://doi.org/10.1002/mame.200500296)
28. Zhang, D.; Wang, Y.; *J Mater. Sci. Eng. B*, **2006**, *134*, 9.
DOI: [10.1016/j.mseb.2006.07.037](https://doi.org/10.1016/j.mseb.2006.07.037)
29. Somani, P. R.; Marimuthu, R.; Mulik, U. P.; Sainkar, S. R.; Amalnerkar, D. P.; *Synth. Met.*, **1999**, *106*, 45.
DOI: [10.1016/S0379-6779\(99\)00081-8](https://doi.org/10.1016/S0379-6779(99)00081-8)
30. Jaidev; Jafri, R. I.; Mishra, A. K.; Ramaprabhu, S.; *J. Mater. Chem.*, **2011**, *21*, 17601.
DOI: [10.1039/C1JM13191E](https://doi.org/10.1039/C1JM13191E)
31. Gupta, N.; Kumar, D.; Tomar, S. K.; *Int. J. Mater. Chem.*, **2012**, *2*, 79.
DOI: [10.5923/j.ijmc.20120202.07](https://doi.org/10.5923/j.ijmc.20120202.07)
32. Ishii, M.; Nakahira, M.; Yamanaka, T.; *Solid State Commun.*, **1972**, *11*, 209.
DOI: [10.1016/0038-1098\(72\)91162-3](https://doi.org/10.1016/0038-1098(72)91162-3)
33. Wang, W. Z.; Xu, C. K.; Wang, G. H.; Liu, Y. K.; Zheng, C. L.; *Adv. Mater.*, **2002**, *14*, 837.
DOI: [10.1002/1521-4095\(20020605\)14:11<837::AID-ADMA837>3.0.CO;2-4](https://doi.org/10.1002/1521-4095(20020605)14:11<837::AID-ADMA837>3.0.CO;2-4)
34. Gupta, N.; Verma, A.; Kashyap, S. C.; Dube, D. C.; *J. Magn. Magn. Mater.*, **2007**, *308*, 137.
DOI: [10.1016/j.jmmm.2006.05.015](https://doi.org/10.1016/j.jmmm.2006.05.015)
35. Durmus, Z.; Baykal, A.; Kavas, H.; Sözeri, H.; *Phys. B*, **2011**, *406*, 1114.
DOI: [10.1016/j.physb.2010.12.059](https://doi.org/10.1016/j.physb.2010.12.059)
36. Hagleitner, C.; Lange, D.; Hierlemann, A.; Brand, O.; Baltes, H.; *IEEE J. Solid-St. Circ.*, **2002**, *37*, 1867.
DOI: [10.1109/JSSC.2002.804359](https://doi.org/10.1109/JSSC.2002.804359)
37. Bai, H.; Shi, G.; *Sens.*, **2007**, *7*, 267.
DOI: [10.3390/s7030267](https://doi.org/10.3390/s7030267)